Structural Aspects and Solution Dynamics of the Auraferraboranes [Fe₄(CO)₁₂Au₂L₂BH]: The Crystal Structures of [Fe₄(CO)₁₂Au₂{P(p-MeC₆H₄)₃}₂BH]·CH₂Cl₂ and [HFe₄(CO)₁₂Au₂{PEt₃}₂B]

Catherine E. Housecroft* and Musa S. Shongwe

University Chemical Laboratory, Lensfield Road, Cambridge CB2 1EW, U.K.

Arnold L. Rheingold*

Department of Chemistry, University of Delaware, Newark, Delaware 19716

Six new auraferraboranes of the general formula [Fe₄(CO)₁₂Au₂LL′BH] (L = L′ = P(c-C₆H₁₁)₃, P(p-MeC₆H₄)₃, PMePh₂, PMe₂Ph, PMe₃; L = PMePh₂, L′ = PMe₂Ph) have been prepared. Two structural types are represented, one in which the endo-hydrogen atom bridges an Fe–B edge (structure I) and one in which it bridges an Fe–Fe edge (structure II). The change in hydrogen atom location is accompanied by a rearrangement of the gold(I) phosphine moieties and a reorientation of one iron tricarbonyl unit, while essentially retaining a constant Fe₄B framework. The crystal structures of two compounds, [Fe₄-(CO)₁₂Au₂{P(p-C₆H₄)₃}₂BH]·CH₂Cl₂ (1) and [HFe₄(CO)₁₂Au₂{PEt₃}₂B] (2), are reported, the former being representative of structure I and the latter of structure II. 1: monoclinic, P2₁/n; a = 20.891 (6), b = 13.367 (4), c = 23.441 (7) Å; β = 110.82 (3)°; V = 6118 (4) Å³; Z = 4; R(F) = 6.39%. 2: monoclinic, I2/a; a = 17.783 (5), b = 11.277 (3), c = 18.084 (7) Å; β = 106.26 (3)°; V = 3481.3 (17) Å³; Z = 4; R(F) = 4.75%. The structure of 1 is similar to that of the related cluster [Fe₄(CO)₁₂Au₂{PPh₃}₂BH] (3). In solution, a ligand-dependent equilibrium exists between structures I and II for the clusters [Fe₄(CO)₁₂Au₂LL′BH]. The factors that control the dominance of structure I or II for a particular phosphine ligand have been investigated, and the interplay of steric and electronic effects has been assessed. Electronic factors appear to drive the gold(I) phosphine groups to interact with Fe–B rather than Fe–Fe edges of the cluster, while steric factors dictate the actual Fe₄Au₂B core geometry.

Recently, we reported the preparation and molecular structure of the metal-rich auraferraborane [Fe₄-(CO)₁₂Au₂{PPh₃}₂BH].[1] This cluster is based upon a tetrairon butterfly framework with a boron atom bonded to all four iron atoms. Since the orbital requirements of a gold(I) phosphine electrophile formally mimic those of a proton,[2] we had anticipated that the Fe₄Au₂BH core structure of [Fe₄(CO)₁₂Au₂{PPh₃}₂BH] would resemble that of the Fe₄BH₃ core of the parent compound [HFe₄(C-O)₁₂BH₂].[3] However, whereas the placement of one AuPPh₃ unit as a bridge across an Fe_wing–B edge was as expected, the observation of the second AuPPh₃ fragment in an Fe_hinge–B edge bridging mode was unprecedented. Instead of distributing themselves over the cluster surface so as to provide two Fe_wing–B edge bridges and one Fe_hinge–Fe_hinge bridge as in the case of [HFe₄(CO)₁₂BH₂], the three electrophiles in [Fe₄(CO)₁₂Au₂{PPh₃}₂BH] are all directly associated with the boron atom. This feature is again observed in the cluster [Fe₄(CO)₁₂Au₃{PPh₃}₃B].[4] After considering the results of a Fenske–Hall molecular orbital analysis of the bonding in [Fe₄(CO)₁₂Au₂-{PPh₃}₂BH],[1] we suggested that the rather unusual metal core geometry observed in this compound may be controlled by the advantages of the gold(I) phosphine fragments bridging Fe–B rather than Fe–Fe edges. In particular, so far as the gold atoms are concerned, a more realistic charge distribution is achieved if the AuPPh₃ fragments interact with the iron–boron edges. However, one point remained unresolved; there are other geometries

available for the Fe₄Au₂B core which are more symmetrical, and thus, presumably, more desirable, than that observed in [Fe₄(CO)₁₂Au₂{PPh₃}₂BH] and in which Fe–(AuL)–B interactions still predominate over Fe–(Au-L)–Fe interactions.

In any system involving phosphine substituents, a change in the ligand will be accompanied by changes in either steric[5] or electronic effects, or both.[6] The competition between these effects has been studied with regard to, for example, associative substitution reactions of transition-metal carbonyl compounds,[7,8] cobalt(II) disproportionation reactions,[9] and control of cluster geometry in [Co₃(μ-R₂P)(CO)₂]₃ (R = Me, Ph, c-C₆H₁₁).[10] However, in transition-metal clusters containing gold(I) phosphine fragments, the extent to which the steric and/or electronic requirements of the phosphine substituent dictate the nature of the product has received little attention. Salter et al. have illustrated that the replacement of two PPh₃ groups for one Ph₂PCH₂CH₂PPh₂ ligand in the compounds [Au₂Ru₄(μ₃-H)(CO)₁₂L₂] and [Au₃Ru₄(μ-H)(CO)₁₂(PPh₃)L₂] (L₂ = (PPh₃)₂ or Ph₂PCH₂CH₂PPh₂) causes structural perturbation.[11,12] The changes in skeletal geometry have been attributed to the relief of steric strain. In a study

(1) Housecroft, C. E.; Rheingold, A. L. *Organometallics* 1987, 6, 1332.
(2) Hall, K. P.; Mingos, D. M. P. *Prog. Inorg. Chem.* 1984, 32, 237.
(3) Fehlner, T. P.; Housecroft, C. E.; Scheidt, W. R.; Wong, K. S. *Organometallics* 1983, 2, 825.
(4) Harpp, K. S.; Housecroft, C. E.; Rheingold, A. L.; Shongwe, M. S. *J. Chem. Soc., Chem. Commun.* 1988, 965.

(5) Tolman, C. A. *Chem. Rev.* 1977, 77, 313.
(6) Rahman, Md. M.; Liu, H. Y.; Prock, A.; Giering, W. P. *Organometallics* 1987, 6, 650.
(7) Dahlinger, K.; Falcone, F.; Poë, A. J. *Inorg. Chem.* 1986, 25, 2654 and references therein.
(8) Poë, A. J. *Pure Appl. Chem.* 1988, 60, 1209.
(9) Socol, S. M.; Verkade, J. G. *Inorg. Chem.* 1986, 25, 2658.
(10) Albright, T. A.; Kang, S.-K.; Afif, A. M.; Bard, A. J.; Jones, R. A.; Leland, J. K.; Schwab, S. T. *Inorg. Chem.* 1988, 27, 1246.
(11) Bates, P. A.; Brown, S. S. D.; Dent, A. J.; Hursthouse, M. B.; Kitchen, G. F. M.; Orpen, A. G.; Salter, I. D.; Sik, V. *J. Chem. Soc., Chem. Commun.* 1986, 600.
(12) Adatia, T.; McPartlin, M.; Salter, I. D. *J. Chem. Soc., Dalton Trans.* 1988, 751.

of steric and electronic factors in some heteronuclear clusters, the consequences of varying the group X in [RuCo$_3$(μ_3-X)(μ-CO)$_3$(CO)$_9$] (X = CuPPh$_3$, AuPPh$_3$, Hg-Co(CO)$_4$, Hg[RuCo$_3$(CO)$_{12}$]) have been analyzed.[13]

In the work reported here, we attempt to analyze the steric and electronic factors that control the geometry of a single heteronuclear cluster core.[14] As we vary the gold-bound ligands L and L' in the compound [Fe$_4$-(CO)$_{12}$Au$_2$LL'BH], we have the opportunity not only to observe changes in site preference of the gold(I) phosphine fragments but also to test our premise that the latter electrophiles tend to aggregate about the boron atom.

Experimental Section

General Data. FT-NMR spectra were recorded on a Bruker WM 250 or AM 400 spectrometer. ^{1}H NMR shifts are reported with respect to δ 0 for Me$_4$Si; ^{11}B NMR with respect to δ 0 for F$_3$B·OEt$_2$; ^{31}P NMR with respect to δ 0 for H$_3$PO$_4$. All downfield chemical shifts are positive. Infrared spectra were recorded on a Perkin-Elmer 983 or FT 1710 spectrophotometer. FAB mass spectra were recorded on a Kratos MS 50TC, MS 902, or MS 890 instrument.

All reactions were carried out under argon by using standard Schlenk techniques. Solvents were dried over suitable reagents and freshly distilled under nitrogen before use. Chromatographic separations were carried out under nitrogen, either by column by using Kieselgel 70–230 mesh (Merck) or by a centrifugal technique by using Kieselgel 60-PF-254 mesh (Merck). Gold(I) phosphines were prepared from HAuCl$_4$ (Aldrich) and P(p-MeC$_6$H$_4$)$_3$, PMe$_2$Ph (Aldrich), PMe$_3$, PMe$_3$, PMePh$_2$, or P(C$_6$H$_{11}$)$_3$ (Strem) by methods based on those reported in the literature.[15,16] The compounds [PPN][HFe$_4$(CO)$_{12}$BH],[17] (PPN = bis(triphenylphosphine)nitrogen(1+)), [HFe$_4$(CO)$_{12}$Au$_2$[PEt$_3$]$_2$B] (2),[18] [Fe$_4$(CO)$_{12}$Au$_2$[PEt$_3$][PPh$_3$]BH],[18] and [Fe$_4$(CO)$_{12}$Au$_2$[PPh$_3$]$_2$BH][1] were prepared as previously reported.

Preparation of [Fe$_4$(CO)$_{12}$Au$_2$[PMePh$_2$]$_2$BH]. In a typical reaction, Au(PMePh$_2$)Cl (0.24 g, 0.55 mmol) was combined with [PPN][HFe$_4$(CO)$_{12}$BH] (0.3 g, 0.27 mmol) in a flask to which CH$_2$Cl$_2$ (30 mL) and TlPF$_6$ (0.2 g, 0.57 mmol) were added. All reagents dissolved to give a red-brown solution, which, after stirring for 45 min, turned green-brown. [PPN][PF$_6$] and TlCl were precipitated by adding Et$_2$O (10 mL). The mixture was filtered and the filtrate evaporated to dryness. After chromatographic separation with CH$_2$Cl$_2$/hexane (1:1) eluent, [Fe$_4$-(CO)$_{12}$Au$_2$[PMePh$_2$]$_2$BH] was obtained as the first, dark green fraction in ca. 70% yield. [Fe$_4$(CO)$_{12}$Au$_2$[PMePh$_2$]$_2$BH]: 250-MHz ^{1}H NMR (CD$_2$Cl$_2$, 293 K) δ 7.8–7.4 (m), 1.91 (d, J_{PH} = 9.3 Hz), –10.6 (br); 128-MHz ^{11}B NMR (CD$_2$Cl$_2$, 295 K) δ 141.8; 162-MHz ^{31}P NMR (CD$_2$Cl$_2$, 295 K) δ 36.2; IR (CH$_2$Cl$_2$, cm^{-1}) ν_{CO} 2058 (m), 2019 (vs), 1996 (vs), 1972 (sh); FAB-MS in 3-NBA matrix, m/z 1366 (P$^+$). Anal. Calcd for Au$_2$BC$_{38}$Fe$_4$H$_{27}$O$_{12}$P$_2$: C, 33.38; H, 1.98. Found: C, 33.48; H, 1.93.

Preparation of [Fe$_4$(CO)$_{12}$Au$_2$[PMe$_2$Ph]$_2$BH]. The procedure was analogous to that described for [Fe$_4$(CO)$_{12}$Au$_2$[PMePh$_2$]$_2$BH], but with a reaction time of 90 min. [Fe$_4$(CO)$_{12}$Au$_2$[PMe$_2$Ph]$_2$BH] was obtained as the first, green-brown fraction in ca. 60% yield. [Fe$_4$(CO)$_{12}$Au$_2$[PMe$_2$Ph]$_2$BH]: 250-MHz ^{1}H NMR (CD$_2$Cl$_2$, 293 K) δ 7.7–7.4 (m), 1.73 (d, J_{PH} = 9.7 Hz), –14.2 (br); 128-MHz ^{11}B NMR (CD$_2$Cl$_2$, 295 K) δ 151.0; 162-MHz ^{31}P NMR (CD$_2$Cl$_2$, 295 K) δ 24.0; IR (CH$_2$Cl$_2$, cm^{-1}) ν_{CO} 2057 (m), 2018 (vs), 1995 (vs), 1971 (sh); FAB-MS in 3-NBA matrix, m/z 1242 (P$^+$).

Preparation of [Fe$_4$(CO)$_{12}$Au$_2$[PMePh$_2$][PMe$_2$Ph]BH]. The procedure was analogous to that descried for [Fe$_4$(CO)$_{12}$Au$_2$-[PMe$_2$Ph]$_2$BH], except that equimolar quantities of Au(PMePh$_2$)Cl

(13) Bender, R.; Braunstein, P.; deMeric de Bellefon, C. *Polyhedron* **1988**, 7, 2271.

(14) A preliminary report has appeared: Housecroft, C. E.; Shongwe, M. S.; Rheingold, A. L. *Organometallics* **1988**, 7, 1885.

(15) Mann, F. G.; Wells, A. F.; Purdie, D. *J. Chem. Soc.* **1937**, 1828.

(16) Williamson, D. R.; Baird, M. C. *J. Inorg. Nucl. Chem.* **1972**, 34, 3393.

(17) Housecroft, C. E.; Buhl, M. L.; Long, G. J.; Fehlner, T. P. *J. Am. Chem. Soc.* **1987**, 109, 3323.

(18) Harpp, K. S.; Housecroft, C. E. *J. Organomet. Chem.* **1988**, 340, 389.

	1	2
	(a) Crystal Parameters	
formula	C$_{50}$H$_{43}$Au$_2$BFe$_4$P$_2$O$_{12}$·CH$_2$Cl$_2$	C$_{24}$H$_{31}$Au$_2$BFe$_4$P$_2$O$_{12}$
cryst system	monoclinic	monoclinic
space group	$P2_1/n$	$I2/a$
a, Å	20.891 (6)^a	17.783 (5)
b, Å	13.367 (4)	11.277 (3)
c, Å	23.441 (7)	18.084 (7)
β, deg	110.82 (3)	106.26 (3)
V, Å^3	6118 (4)	3481.3 (17)
Z	4	4
D(calcd), g cm^{-3}	1.748	2.293
mol wt	1610.9	1201.6
μ(Mo Kα), cm^{-1}	58.9	101.5
cryst color	brown black	black
cryst size, mm	0.15 × 0.25 × 0.28	0.28 × 0.28 × 0.33
temp, K	292	296
	(b) Data Collection	
scan limits, deg	$4 \le 2\theta \le 47$	$4 \le 2\theta \le 55$
rflns collected	9461	4333
indpt rflns	8927	4001
obs rflns ($5\sigma(F_o)$)	5119	2965
R(merge), %	0.98	2.1
T_{max}/T_{min}	2.82	4.52
decay, %	≤ 1	≤ 5
	(c) Refinement	
$R(F)$, $R(wF)$, %	6.39, 5.97	4.75, 6.03
GOF	1.387	1.344
Δ/σ(final)	0.083	0.047
$\Delta(\rho)_{max}$, e Å^{-3}	3.92	2.62
N_o/N_v	7.33	14.46
g, $w^{-1} = \sigma^2(F_o) + gF_o^2$	0.001	0.001

^{a}Unit-cell parameters determined from the least-squares fit of the angular settings of 25 reflections (22° $\le 2\theta \le$ 27°).

and Au(PMe$_2$Ph)Cl were used in the reaction. Both [Fe$_4$-(CO)$_{12}$Au$_2$[PMe$_2$Ph]$_2$BH] and [Fe$_4$(CO)$_{12}$Au$_2$[PMePh$_2$]BH] were obtained in addition to the desired [Fe$_4$(CO)$_{12}$Au$_2$[PMePh$_2$]-[PMe$_2$Ph]BH]. It was not possible to separate these three products, and the spectral characteristics of [Fe$_4$(CO)$_{12}$Au$_2$-[PMePh$_2$][PMe$_2$Ph]BH] were assigned by comparison of spectra of the mixture with those of pure [Fe$_4$(CO)$_{12}$Au$_2$[PMePh$_2$]$_2$BH] and pure [Fe$_4$(CO)$_{12}$Au$_2$[PMe$_2$Ph]$_2$BH]. [Fe$_4$(CO)$_{12}$Au$_2$-[PMePh$_2$][PMe$_2$Ph]BH]: 250-MHz ^{1}H NMR (CD$_2$Cl$_2$, 293 K) δ 7.8–7.4 (m), 2.03 (d, J_{PH} = 9.3 Hz, PPh$_2$Me), 1.61 (d, J_{PH} = 9.8 Hz, PPhMe$_2$), –12.1 (br); 128-MHz ^{11}B NMR (CD$_2$Cl$_2$, 295 K) δ 145.5; 162-MHz ^{31}P NMR (CD$_2$Cl$_2$, 295 K) δ 25.0; IR (CH$_2$Cl$_2$, cm^{-1}) ν_{CO} 2058 (m), 2019 (vs), 1996 (vs), 1972 (sh); FAB-MS in 3-NBA matrix, m/z 1304 (P$^+$).

Preparation of [Fe$_4$(CO)$_{12}$Au$_2$[P(p-MeC$_6$H$_4$)$_3$]$_2$BH]·CH$_2$Cl$_2$ (1). The reaction procedure was analogous to that described for the preparation of [Fe$_4$(CO)$_{12}$Au$_2$[PMePh$_2$]$_2$BH]. [Fe$_4$-(CO)$_{12}$Au$_2$[P(p-MeC$_6$H$_4$)$_3$]$_2$BH] was obtained as the second, dark green, fraction in ca. 90% yield. Crystals suitable for X-ray analysis were grown from CH$_2$Cl$_2$ layered with petroleum ether (40–60) and hexane. [Fe$_4$(CO)$_{12}$Au$_2$[P(p-MeC$_6$H$_4$)$_3$]$_2$BH]: 250-MHz ^{1}H NMR (CD$_2$Cl$_2$, 293 K) δ 7.5–7.0 (m), 2.34 (s), –9.1 (br); 128-MHz ^{11}B NMR (CD$_2$Cl$_2$, 295 K) δ 138.0; 162-MHz ^{31}P NMR (CD$_2$Cl$_2$, 295 K) δ 49.0; IR (CH$_2$Cl$_2$, cm^{-1}) ν_{CO} 2056 (m), 2018 (vs), 1994 (vs), 1970 (sh); FAB-MS in 3-NBA matrix, m/z 1574 (P$^+$). Anal. Calcd for Au$_2$BC$_{55}$Cl$_2$Fe$_4$H$_{45}$O$_{12}$P$_2$: C, 39.78; H, 2.71. Found: C, 39.52; H, 2.94.

Preparation of [Fe$_4$(CO)$_{12}$Au$_2$[P(c-C$_6$H$_{11}$)$_3$]$_2$BH]·CH$_2$Cl$_2$. The reaction procedure was analogous to that described for the preparation of [Fe$_4$(CO)$_{12}$Au$_2$[PMePh$_2$]$_2$BH]. [Fe$_4$(CO)$_{12}$Au$_2$[P-(c-C$_6$H$_{11}$)$_3$]$_2$BH] was obtained as the second, dark green, fraction in ca. 15% yield. [Fe$_4$(CO)$_{12}$Au$_2$[P(c-C$_6$H$_{11}$)$_3$]$_2$BH]: 250-MHz ^{1}H NMR (CD$_2$Cl$_2$, 293 K) δ 0.85–1.95 (m), –9.1 (br); 128-MHz ^{11}B NMR (CD$_2$Cl$_2$, 298 K) δ 140.0; 162-MHz ^{31}P NMR (CD$_2$Cl$_2$, 298 K) δ 66.0; IR (CH$_2$Cl$_2$, cm^{-1}) ν_{CO} 2055 (m), 2015 (vs), 1991 (vs), 1970 (sh); FAB-MS in 3-NBA matrix, m/z 1526 (P$^+$). Anal. Calcd for Au$_2$BC$_{49}$Cl$_2$Fe$_4$H$_{69}$O$_{12}$P$_2$: C, 36.50; H, 4.28. Found: C, 36.78; H, 4.32.

Table II. Atomic Coordinates ($\times 10^4$) and Isotropic Thermal Parameters ($\text{Å}^2 \times 10^3$) for
$[Fe_4(CO)_{12}Au_2\{P(p\text{-}MeC_6H_4)_3\}_2BH]\cdot CH_2Cl_2$

	x	y	z	U		x	y	z	U
Au(1)	7595.0 (4)	7671.2 (5)	-38.3 (3)	36.1 (3)[a]	C(27)	5000 (10)	3798 (15)	-671 (10)	72 (11)[a]
Au(2)	6258.4 (4)	8728.1 (5)	-551.7 (3)	37.0 (3)[a]	C(31)	8814 (7)	4866 (11)	-65 (5)	60 (10)[a]
Fe(1)	8254 (1)	9050 (2)	757 (1)	43 (1)[a]	C(32)	9321	4299	363	91 (13)[a]
Fe(2)	6920 (1)	8686 (2)	633 (1)	35 (1)[a]	C(33)	9341	4235	963	71 (11)[a]
Fe(3)	7912 (2)	10273 (2)	-214 (1)	55 (1)[a]	C(34)	8853	4738	1135	51 (9)[a]
Fe(4)	7448 (1)	10539 (2)	701 (1)	42 (1)[a]	C(35)	8346	5305	708	65 (10)[a]
P(1)	7628 (3)	6095 (3)	-429 (2)	38 (2)[a]	C(36)	8327	5369	108	39 (8)[a]
P(2)	5390 (2)	8630 (3)	-1500 (2)	35 (2)[a]	C(37)	9838 (12)	3602 (20)	1412 (11)	126 (16)[a]
B	7305 (12)	9359 (13)	59 (8)	39 (9)[a]	C(41)	7538 (6)	5218 (8)	-1537 (6)	59 (10)[a]
C(1)	8463 (9)	8008 (13)	1270 (8)	51 (8)[a]	C(42)	7702	5155	-2062	68 (11)[a]
O(1)	8619 (8)	7350 (10)	1598 (6)	80 (7)[a]	C(43)	8100	5899	-2191	53 (9)[a]
C(2)	8960 (13)	8767 (16)	536 (10)	85 (13)[a]	C(44)	8333	6706	-1793	70 (12)[a]
O(2)	9418 (9)	8563 (14)	398 (9)	123 (11)[a]	C(45)	8168	6769	-1267	51 (9)[a]
C(3)	8619 (12)	9961 (15)	1356 (10)	64 (11)[a]	C(46)	7771	6025	-1139	43 (8)[a]
O(3)	8948 (8)	10388 (11)	1773 (7)	97 (8)[a]	C(47)	8273 (13)	5818 (19)	-2755 (10)	109 (15)[a]
C(4)	6699 (11)	7379 (15)	621 (8)	54 (10)[a]	C(51)	6319 (6)	7888 (10)	-2009 (5)	64 (10)[a]
O(4)	6559 (9)	6567 (11)	648 (7)	85 (9)[a]	C(52)	6534	7648	-2492	84 (13)[a]
C(5)	7287 (10)	8645 (14)	1464 (10)	53 (10)[a]	C(53)	6114	7860	-3091	74 (12)[a]
O(5)	7499 (8)	8581 (11)	1982 (6)	77 (7)[a]	C(54)	5478	8312	-3208	76 (12)[a]
C(6)	6095 (10)	9170 (14)	589 (7)	49 (8)[a]	C(55)	5262	8552	-2725	47 (8)[a]
O(6)	5553 (7)	9379 (12)	554 (7)	87 (8)[a]	C(56)	5682	8340	-2126	38 (8)[a]
C(7)	7358 (12)	10718 (14)	1416 (10)	69 (11)[a]	C(57)	6331 (13)	7562 (19)	-3614 (11)	111 (16)[a]
O(7)	7276 (9)	10904 (11)	1877 (7)	88 (9)[a]	C(61)	4536 (6)	6986 (10)	-1957 (4)	45 (8)[a]
C(8)	6630 (11)	10986 (13)	226 (8)	45 (9)[a]	C(62)	4026	6309	-1963	58 (9)[a]
O(8)	6122 (8)	11310 (10)	-77 (7)	73 (8)[a]	C(63)	3742	6348	-1507	59 (9)[a]
C(9)	7882 (11)	11730 (15)	783 (9)	64 (10)[a]	C(64)	3968	7063	-1046	58 (10)[a]
O(9)	8113 (9)	12513 (10)	824 (9)	110 (10)[a]	C(65)	4479	7741	-1040	54 (9)[a]
C(10)	7522 (12)	11383 (14)	-606 (10)	74 (12)[a]	C(66)	4763	7702	-1495	40 (7)[a]
O(10)	7248 (9)	12087 (10)	-859 (7)	93 (9)[a]	C(67)	3194 (12)	5610 (17)	-1476 (11)	103 (14)[a]
C(11)	8734 (11)	10822 (16)	200 (12)	87 (13)[a]	C(71)	4215 (6)	9805 (8)	-2057 (5)	41 (8)[a]
O(11)	9228 (9)	11223 (14)	371 (9)	132 (12)[a]	C(72)	3878	10711	-2254	59 (9)[a]
C(12)	8185 (13)	9715 (15)	-762 (12)	80 (14)[a]	C(73)	4242	11608	-2114	63 (11)[a]
O(12)	8313 (11)	9351 (13)	-1155 (9)	117 (12)[a]	C(74)	4943	11599	-1777	75 (13)[a]
C(21)	6889 (6)	4353 (8)	-380 (6)	62 (11)[a]	C(75)	5280	10692	-1579	49 (9)[a]
C(22)	6291	3832	-436	56 (10)[a]	C(76)	4916	9795	-1720	35 (4)
C(23)	5663	4329	-629	49 (9)[a]	C(77)	3882 (14)	12607 (16)	-2332 (12)	116 (17)[a]
C(24)	5633	5347	-767	57 (10)[a]	Cl(1)	4049 (8)	6345 (8)	2256 (7)	239 (10)[a]
C(25)	6231	5868	-711	70 (12)[a]	Cl(2)	4405 (10)	4815 (17)	3102 (10)	348 (17)[a]
C(26)	6859	5371	-518	36 (8)[a]	C(s)	4390 (19)	5023 (30)	2437 (17)	253 (33)[a]

[a] Equivalent isotropic U defined as one-third of the trace of the orthogonalized U_{ij} tensor.

Preparation of $[Fe_4(CO)_{12}Au_2\{PMe_3\}_2BH]$. The reaction procedure was analogous to that described for the preparation of $[Fe_4(CO)_{12}Au_2\{PMePh_2\}_2BH]$. $[Fe_4(CO)_{12}Au_2\{PMe_3\}_2BH]$ was obtained as the first, brown-green, fraction in ca. 50% yield. $[Fe_4(CO)_{12}Au_2\{PMe_3\}_2BH]$: 250-MHz ^1H NMR (CD_2Cl_2, 293 K) δ 1.72 (d, J_{PH} = 8.7 Hz), -17.8 (br); 128-MHz ^{11}B NMR (CD_2Cl_2, 295 K) δ 163.8; 162-MHz ^{31}P NMR (CD_2Cl_2, 295 K) δ 7.5; IR (CH_2Cl_2, cm^{-1}) ν_{CO} 2054 (m), 2015 (vs), 1992 (vs), 1970 (sh); FAB-MS in 3-NBA matrix, m/z 1118 (P$^+$).

Crystal Structural Determinations. General Data. Crystallographic data are collected in Table I. A Nicolet R3m diffractometer, using graphite-monochromated Mo Kα radiation (λ = 0.710 73 Å), was used for the data collections by the Wyckoff method. All non-hydrogen atoms were anisotropically refined, and all hydrogen atoms (except for the hydrido atoms) were treated as idealized contributions (d(C–H) = 0.96 Å). All computations used the SHELXTL 5.1 program library (G. Sheldrick, Nicolet Corp., Madison, WI).

$[Fe_4(CO)_{12}Au_2\{P(p\text{-}MeC_6H_4)_3\}_2BH]\cdot CH_2Cl_2$ (1). An irregularly shaped specimen of 1 was mounted in epoxy cement. Photographic characterization revealed monoclinic symmetry, and systematic absences in the data determined that the space group was $P2_1/n$. The absorption correction was based on seven Ψ-scan reflections (10° steps, 21° ≤ 2θ ≤ 35°); R(merge) for these 252 data was reduced from 17.9 to 5.5%. The structure was solved by direct methods that located the six metal atoms. Refinement revealed the presence of a molecule of recrystallization solvent, CH_2Cl_2, for each cluster molecule. The six tolyl rings were fixed to rigid hexagonal structures. Table II contains the atomic coordinates for 1, and Table III contains selected bond distances and angles. Tables of atomic coordinates, bond distances and angles, thermal parameters, H-atom fractional coordinates, and structure factor amplitudies are available as supplementary

material (see pargraph at the end of the paper).

$[HFe_4(CO)_{12}Au_2\{PEt_3\}_2B]$ (2). Crystals of 2 were mounted in epoxy cement. Photographic characterization revealed monoclinic symmetry. Systematic absences in the data determined either of the space groups $I2/a$ or Ia. The former was initially suggested by the distribution of the E statistics and later confirmed by the presence of a crystallographic 2-fold axis (located at the midpoints of the Au–Au(a) and Fe(1)–Fe(1a) vectors and passing through the B atom). The data were corrected for absorption based on six Ψ-scan reflections (216 data, 10° increments, 20° ≤ 2θ ≤ 31°). The unique Au atom was located by heavy-atom methods. Table IV contains the atomic coordinates for 2, and Table V contains selected bond distances and angles. Tables of atomic coordinates, bond distances and angles, thermal parameters, H-atom coordinates, and structure factor amplitudes are available as supplementary material in ref 14.

Results and Discussion

Molecular Structure of 1. The molecular structure of 1 is shown in Figure 1, and selected bond length and angle data are given in Table III. A determination of the molecular structure of 1 was of interest to us for comparative purposes with the structure of $[Fe_4(CO)_{12}Au_2\{PPh_3\}_2BH]$ (3).[1] One of our aims was to probe the extent to which the increase in σ-donor ability in going from PPh_3 to $P(p\text{-}MeC_6H_4)_3$, while maintaining a constant phosphine cone angle[5,19] (θ = 145°), influenced the site preference of the gold(I) phosphine moiety. In the event, the structure of 1 bears a striking resemblance to that of 3[1] and exhibits

(19) Tolman, C. A. *J. Am. Chem. Soc.* **1970**, *92*, 2956.

Table III. Selected Bond Distances and Angles for [Fe₄(CO)₁₂Au₂{P(p-MeC₆H₄)₃}₂BH]•CH₂Cl₂

(a) Bond Distances (Å)

Au(1)–Au(2)	2.975 (1)	Fe(1)–Fe(2)	2.685 (4)
Au(1)–Fe(1)	2.635 (2)	Fe(1)–Fe(4)	2.580 (4)
Au(1)–Fe(2)	2.808 (3)	Fe(1)–B	2.114 (19)
Au(1)–P(1)	2.308 (5)	Fe(2)–Fe(4)	2.692 (3)
Au(1)–B	2.368 (18)	Fe(2)–B	2.008 (24)
Au(2)–Fe(2)	2.627 (2)	Fe(3)–Fe(4)	2.674 (5)
Au(2)–P(2)	2.319 (4)	Fe(3)–B	2.024 (24)
Au(2)–B	2.306 (20)	Fe(4)–B	2.126 (19)
Fe(1)–Fe(2)	2.741 (4)		

(b) Bond Angles (deg)

Au(2)–Au(1)–Fe(1)	97.7 (1)	Fe(1)–Fe(2)–Fe(4)	56.7 (1)
Au(2)–Au(1)–Fe(2)	53.9 (1)	Au(1)–Fe(2)–B	56.0 (6)
Fe(1)–Au(1)–Fe(2)	60.4 (1)	Au(2)–Fe(2)–B	57.8 (5)
Au(2)–Au(1)–P(1)	115.4 (1)	Fe(1)–Fe(2)–B	50.0 (6)
Fe(1)–Au(1)–P(1)	146.9 (1)	Fe(4)–Fe(2)–B	51.3 (5)
Fe(2)–Au(1)–P(1)	139.0 (2)	Fe(1)–Fe(3)–Fe(4)	57.6 (1)
Au(2)–Au(1)–B	49.5 (5)	Fe(1)–Fe(3)–B	51.0 (5)
Fe(1)–Au(1)–B	49.6 (4)	Fe(4)–Fe(3)–B	51.6 (6)
Fe(2)–Au(1)–B	44.7 (6)	Fe(1)–Fe(4)–Fe(2)	62.6 (1)
P(1)–Au(1)–B	162.3 (4)	Fe(1)–Fe(4)–Fe(3)	61.4 (1)
Au(1)–Au(2)–Fe(2)	59.8 (1)	Fe(2)–Fe(4)–Fe(3)	95.1 (1)
Au(1)–Au(2)–P(2)	131.5 (1)	Fe(1)–Fe(4)–B	52.3 (5)
Fe(2)–Au(2)–P(2)	161.9 (2)	Fe(2)–Fe(4)–B	47.5 (6)
Au(1)–Au(2)–B	51.4 (5)	Fe(3)–Fe(4)–B	48.2 (7)
Fe(2)–Au(2)–B	47.5 (6)	Au(1)–B–Fe(1)	71.8 (6)
P(2)–Au(2)–B	149.5 (5)	Fe(2)–Fe(4)–C(7)	90.1 (6)
Au(1)–Fe(1)–Fe(2)	62.9 (1)	Au(1)–B–Fe(2)	79.4 (6)
Au(1)–Fe(1)–Fe(3)	84.9 (1)	Au(1)–B–Au(2)	79.1 (5)
Fe(2)–Fe(1)–Fe(3)	93.7 (1)	Fe(1)–B–Fe(2)	83.3 (7)
Au(1)–Fe(1)–Fe(4)	109.6 (1)	Au(2)–B–Fe(1)	146.2 (9)
Fe(2)–Fe(1)–Fe(4)	60.7 (1)	Au(2)–B–Fe(3)	125.9 (9)
Fe(3)–Fe(1)–Fe(4)	61.0 (1)	Au(2)–B–Fe(2)	74.7 (8)
Au(1)–Fe(1)–B	58.6 (5)	Fe(2)–B–Fe(3)	158.2 (10)
Fe(2)–Fe(1)–B	46.7 (7)	Au(1)–B–Fe(3)	109.5 (11)
Fe(3)–Fe(1)–B	48.1 (6)	Au(2)–B–Fe(4)	125.1 (11)
Fe(4)–Fe(1)–B	52.7 (5)	Fe(1)–B–Fe(3)	80.9 (8)
Au(1)–Fe(2)–Au(2)	66.3 (1)	Fe(2)–B–Fe(4)	81.2 (8)
Au(1)–Fe(2)–Fe(1)	104.0 (1)	Fe(1)–B–Fe(4)	75.0 (6)
Au(1)–Fe(2)–Fe(4)	101.6 (1)	Fe(3)–B–Fe(4)	80.2 (7)
Au(2)–Fe(2)–Fe(4)	95.3 (1)		

Table IV. Atomic Coordinates (×10⁴) and Isotropic Thermal Parameters (Å² × 10³) for [HFe₄(CO)₁₂Au₂{PEt₃}₂B]

	x	y	z	U
Au	6994.3 (2)	2291.1 (4)	4223.3 (2)	54.4 (1)[a]
Fe(1)	6767.3 (7)	–671 (1)	4582.4 (8)	50.9 (4)[a]
Fe(2)	7843.1 (7)	470 (1)	4057.6 (8)	49.9 (4)[a]
P	6166 (2)	3844 (3)	3754 (2)	58.3 (9)[a]
B	7500	744 (13)	5000	49 (5)[a]
O(1)	7013 (6)	1284 (9)	2517 (5)	91 (4)[a]
O(2)	5950 (6)	–2683 (7)	5018 (6)	87 (4)[a]
O(3)	5293 (5)	594 (9)	4052 (8)	116 (5)[a]
O(4)	6646 (6)	–1720 (10)	3071 (5)	96 (4)[a]
O(5)	9159 (6)	2076 (10)	4265 (6)	103 (5)[a]
O(6)	8568 (5)	–1443 (8)	3397 (5)	86 (4)[a]
C(1)	7307 (6)	1019 (10)	3124 (6)	60 (4)[a]
C(2)	6258 (6)	–1877 (9)	4861 (6)	60 (4)[a]
C(3)	5872 (7)	147 (10)	4251 (7)	72 (4)[a]
C(4)	6748 (7)	–1289 (11)	3647 (7)	73 (4)[a]
C(5)	8642 (7)	1486 (11)	4186 (6)	71 (4)[a]
C(6)	8284 (6)	–743 (10)	3671 (6)	59 (4)[a]
C(7)	5330 (6)	3851 (11)	4128 (7)	69 (4)[a]
C(8)	4692 (8)	4802 (13)	3782 (8)	91 (6)[a]
C(9)	5768 (8)	3781 (12)	2719 (7)	79 (5)[a]
C(10)	5270 (8)	2690 (14)	2435 (8)	92 (6)[a]
C(11)	6616 (8)	5291 (11)	3948 (8)	84 (6)[a]
C(12)	7365 (8)	5421 (14)	3732 (10)	99 (7)[a]

[a] Equivalent isotropic U defined as one third of the trace of the orthogonalized U_{ij} tensor.

an asymmetrical array of six metal atoms surrounding a boron atom. Each AuP(p-MeC₆H₄)₃ fragment bridges one Fe–B edge of the tetrairon butterfly framework; Au(2) is associated with the wingtip Fe(2) atom, while Au(1) in-

Table V. Selected Bond Distances Angles (deg) for [HFe₄(CO)₁₂Au₂{PEt₃}₂B]

(a) Bond Distances (Å)

Au–Fe(2)	2.615 (1)	Fe(2)–B	1.989 (3)
Au–Au(a)	2.880 (1)	Fe(1)–C(2)	1.783 (11)
Au–P	2.293 (3)	Fe(1)–C(3)	1.792 (11)
Fe(1)–Fe(2)	2.690 (2)	Fe(1)–C(4)	1.822 (13)
Fe(1)–Fe(2a)	2.689 (2)	Fe(2)–C(1)	1.799 (10)
Fe(1)–Fe(1a)	2.621 (2)	Fe(2)–C(5)	1.789 (13)
Fe(1)–B	2.065 (11)	Fe(2)–C(6)	1.811 (11)

(a) Bond Angles (deg)

Fe(2)–Au–P	152.8 (1)	Au–Fe(2)–Fe(1a)	106.3 (1)
Fe(2)–Au–B	47.4 (1)	Fe(1)–Fe(2)–Fe(1a)	58.3 (1)
P–Au–B	157.1 (1)	B–Fe(2)–Fe(1a)	49.7 (3)
Fe(2)–Au–Au(a)	83.6 (1)	Au–B–Fe(1)	105.6 (1)
P–Au–Au(a)	121.5 (1)	Au–B–Fe(2)	75.6 (1)
B–Au–Au(a)	50.5 (2)	Fe(1)–B–Fe(2)	83.1 (3)
Fe(2)–Fe(1)–B	47.2 (1)	Fe(1a)–Fe(1)–Fe(2a)	60.9 (1)
Fe(1)–B–Au(a)	157.4 (1)	Fe(2)–Fe(1)–Fe(1a)	60.8 (1)
B–Fe(1)–Fe(1a)	50.6 (3)	Fe(2)–B–Au(a)	119.2 (4)
Au–B–Fe(1a)	157.4 (1)	Fe(2)–Fe(1)–Fe(2a)	93.9 (1)
B–Fe(1)–Fe(2a)	47.2 (1)	Fe(1)–B–Fe(1a)	78.8 (5)
Au–B–Au(a)	79.1 (5)	Fe(2)–B–Fe(1a)	83.1 (3)
Au–Fe(2)–Fe(1)	81.1 (1)	Fe(1)–B–Fe(2a)	83.1 (3)
Au–Fe(2)–B	56.9 (3)	Fe(2)–B–Fe(2a)	162.1 (8)
Fe(1)–Fe(2)–B	49.7 (3)		
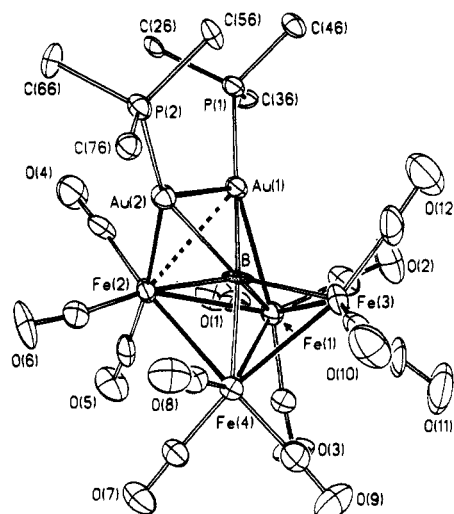
Figure 1. Molecular structure and labeling scheme for **1**. The p-tolyl groups are depicted as ipso-carbon atoms only.

teracts with the hinge Fe(1) atom. The interatomic distances observed in thse three-center Fe–Au–B interactions are compatible with those previously noted in **3**; viz., Fe(2)–Au(2) = 2.627 (2) and Au(2)–B = 2.306 (20) Å as compared to 2.606 (1) and 2.35 (1) Å in **3**, and Fe(1)–Au(1) = 2.635 (2) and Au(1)–B = 2.368 (18) Å as compared to 2.630 (1) and 2.36 (1) Å in **3**.[1] There are no significant differences between the Au–P distances in **1** and **3**, despite the greater σ-donor capacity of P(p-MeC₆H₄)₃ with respect to PPh₃.

The two sets of carbonyl ligands attached to the two hinge iron atoms are asymmetrically disposed; one set is ≈60° out of phase with the second set. Thus, as in **3**,[1] the axial carbonyl ligand C(3)O(3), attached to the hinge iron atom Fe(1), leans over in a semibridging mode toward Fe(4), while the two equatorial CO ligands C(1)O(1) and C(2)O(2) make room for the bulky AuP(p-MeC₆H₄)₃ group that bridges the Fe(1)–B edge.

In **1**, the cluster-bound hydrogen atom was not located. However, the observations in the ¹¹B NMR spectrum of ¹¹B–¹H spin coupling ($J_{BH} \approx 75$ Hz) and in the ¹H NMR spectrum of a broad signal at δ –9.1 are consistent with the placement of a proton along an Fe–H–B edge. Inspection

Table VI. Comparative Geometric Parameters for the Fe_4B Core of 1 and 2 and Some Related Ferraboranes

compound	internal dihedral angle of Fe_4 butterfly, deg	height of B atom above Fe_{wing}–Fe_{wing} axis, Å	ref
$[HFe_4(CO)_{12}BH_2]$	114.0	0.31	3
$[Fe_4(CO)_{12}Au_2\{PPh_3\}_2BH]$	113.4 (3)	0.37 (1)	1
$[Fe_4(CO)_{12}Au_2\{P(p\text{-}MeC_6H_4)_3\}_2BH]$	113.3 (3)	0.38 (1)	a
$[HFe_4(CO)_{12}Au_2\{PEt_3\}_2B]$	113.5 (3)	0.31 (1)	14, a

a This work.
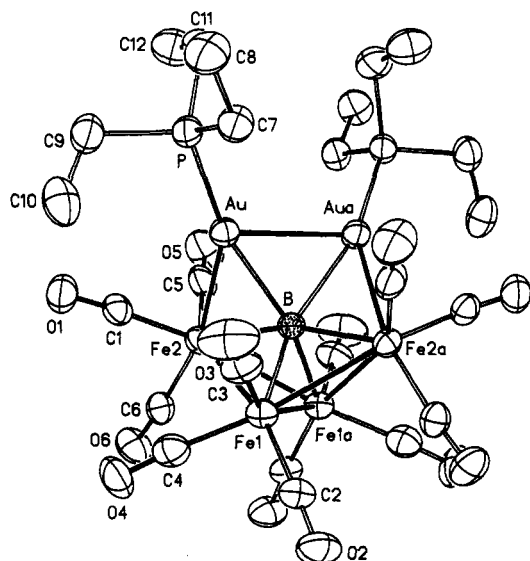
Figure 2. Molecular structure and labeling scheme for 2. The ethyl groups are depicted as ipso-carbon atoms only.

(a)   (b)

Figure 3. Corresponding views of (a) $[HFe_4(CO)_{12}Au_2\{PEt_3\}_2B]$ and (b) $[Fe_4(CO)_{12}Au_2\{PEt_3\}_2C]^{21}$ showing respectively the distortion away from and the adherence to an octahedral Fe_4Au_2 core.

of Figure 1, and in particular of the carbonyl ligand arrangement therein, suggests that the proton bridges the Fe(3)–B edge. This result mimics that found for compound 3.

Molecular Structure of 2. The molecular structure of 2 is shown in Figure 2, and selected bond distance and angle data are given in Table V. Unlike the structures of 1 and 3, that of 2 possesses a C_2 axis passing through the boron atom and the center of the hinge bond of the tetrairon butterfly skeleton. With respect to 1 and 3, the higher symmetry of 2 has several ramifications. First, both the gold(I) phosphine electrophiles bridge the same type of Fe–B edge; viz., Fe_{wing}–Au(PEt₃)–B interactions exist. Second, the two sets of hinge associated carbonyl ligands are related by the C_2 axis, and a semibridging carbonyl ligand cannot be, and, indeed, is not, observed across the iron hinge bond. Third, the endo-hydrogen atom in 2 cannot bridge an Fe_{wing}–B edge. The hydrogen atom was not located crystallographically, but the symmetry requirements of the cluster, and the observed carbonyl ligand distribution (Figure 2), imply that it is hydridic in nature and bridges Fe(1)–Fe(1a).

The boron atom in 2 interacts with all six atoms of the metal framework and lacks a boron–hydrogen interaction. Thus, the cluster should be classed as a metal boride. It is, perhaps, odd that the cluster does not attain a regular octahedral geometry. This feature is emphasized in Figure 3a. Compound 2 is isoelectronic with the carbide cluster $Fe_4(CO)_{12}Au_2\{PEt_3\}_2C$, the metal core of which is virtually octahedral (Figure 3b).[20,21] Hence, it seems unlikely that steric strain between the ethyl substituents of the PEt₃ groups and the axial carbonyl ligands on the hinge Fe
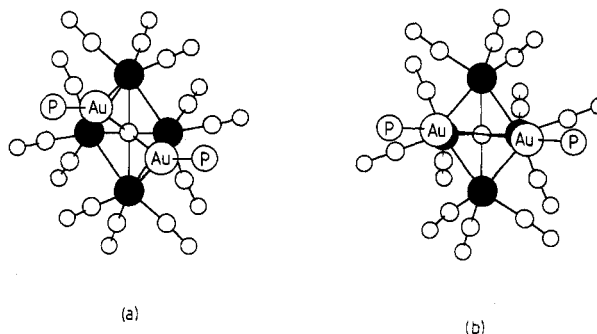
atoms prevents the more regular geometry from forming. Cluster 2 differs from $[Fe_4(CO)_{12}Au_2\{PEt_3\}_2C]$ in having an endo-hydrogen atom. A complete assessment of the role that this proton plays in determining the geometry of the hexametal atom skeleton must await a crystallographic investigation of the anion $[Fe_4(CO)_{12}Au_2\{PEt_3\}_2B]^-$.

Finally, it is notable that the Fe_4B core of compounds 1, 2, and 3 is of an invariant geometry and experiences negligible perturbation in going from the parent ferraborane $[HFe_4(CO)_{12}BH_2]$ to the digold derivatives. Table VI lists the tetrairon butterfly internal dihedral angle and the height of the boron atom above a line joining two of the wing-tip atoms of the butterfly for each compound. The consistency of the parameters is quite remarkable. We may view the $Fe_4(CO)_{12}B$ fragment as a framework upon which electrophilic substitutions occur and which, apart from carbonyl ligand reorientations, is quite resistant to change.

Solution Structure of 2. Previously,[18] we reported that solution spectroscopic data for 2 were consistent with a structure analogous to that determined for 3. Indeed, at room temperature, compound 2 exhibits a broad resonance in the ¹H NMR spectrum at δ −10.4 and, in the ¹¹B NMR spectrum, shows a singlet at δ 142.4 which sharpens slightly in the ¹¹B{¹H} NMR spectrum. We considered that these data were sufficiently similar to those of 3 (viz. a ¹H NMR resonance at δ −9.1 and an ¹¹B NMR signal at δ 137.7)[1,18] to imply analogous structures. In addition, in both compounds, low-temperature 162-MHz ³¹P NMR spectra[18] indicated *two* phosphorus environments, in keeping with the solid-state structure known for 3. The results of the crystallographic determination of 2 described above naturally aroused our curiosity. Not only was there a single phosphorus environment but also the static structure implied the presence of a metal hydride, Fe–H–Fe, rather than an Fe–H–B bridge. In addition, the molecular structure of 2 illustrated a fully metal-encapsulated boron atom; such an environment should be reflected by an ¹¹B NMR spectral shift further downfield than that observed at δ 142.4.[4,22]

The results of a variable-temperature ¹H NMR spectroscopic study on 2 are illustrated in Figure 4. The

(20) Johnson, B. F. G.; Kaner, D. A.; Lewis, J.; Raithby, P. R.; Rosales, M. J. *J. Organomet. Chem.* **1982,** *231,* C59.

(21) Coordinates for $[Fe_4(CO)_{12}Au_2\{PEt_3\}_2C]$ were obtained from P. R. Raithby, private communication.

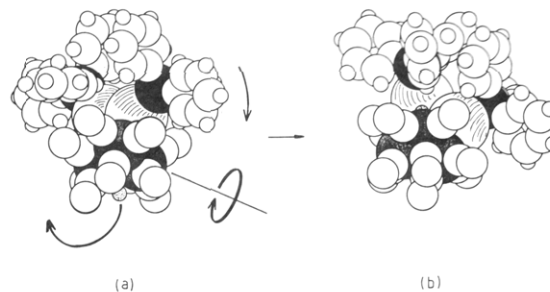(22) Fehlner, T. P.; Rath, N. P. *J. Am. Chem. Soc.* **1988,** *110,* 5345.
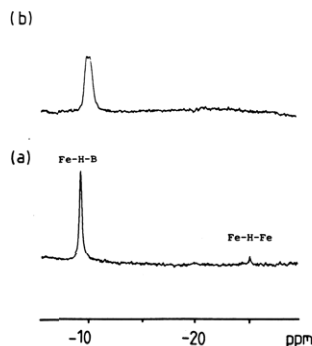
Figure 4. 250-MHz ^{1}H NMR spectra for **2**, plotted in the region of Fe–H–B and Fe–H–Fe resonances, at (a) 200 K and (b) 298 K. The sharpening of the resonance attributed to the Fe–H–B proton is due to thermal ^{11}B–^{1}H spin decoupling.

Figure 5. Space-filling diagram of isomer II of HFe$_4$(CO)$_{12}$Au$_2$[PEt$_3$]$_2$B, viewed along the iron butterfly wing–wing axis. The ethyl groups are oriented as determined from the X-ray diffraction data.

appearance, on cooling, of a metal hydride signal at δ–24.9 is, perhaps, less convincing than the shift of the signal due to the Fe–H–B bridging proton from δ –10.4 to δ –9.1.[23] These data indicate the presence of two isomers of **2** in solution.[24] The major isomer has, as we originally postulated,[18] a structure analogous to **3** (structure I) while the minor isomer has the structure illustrated in Figure 2 (structure II). The ^{1}H NMR chemical shift data suggest that, for **2**, isomer II is present in CH$_2$Cl$_2$ solution to an extent of only $\approx$8%. For both the isomers to be observed by using NMR spectroscopy, the energy difference between them must be small. In the solid state, crystal-packing forces may be responsible for altering the preference between structures I and II. To test this, crystals of **2** were dissolved at 200 K, and a ^{1}H NMR spectrum immediately recorded. The intensity of the hydride signal relative to that shown in Figure 4a increased, but only to the extent of indicating that the ratio of isomers I:II was now $\approx$5:1.

Comparison of Structures I and II. Figure 5 shows a space-filling diagram of isomer II of compound **2**. The ethyl substituents are well separated from each other and from the carbonyl ligands of the Fe$_4$(CO)$_{12}$ framework; interphosphine P···P = 5.40 Å, shortest *interphosphine* H···H = 2.58 Å compared to a shortest *intraphosphine* H···H = 2.50 Å, and shortest H···OC$_{hinge}$ = 2.83 Å and H···OC$_{wing}$ = 2.68 Å. In compounds **1** and **3**, the interphosphine P···P separations are 5.59 and 5.31 Å, respectively. Since the P···P distances are similar in all three compounds, it might appear that structure II could, on steric grounds, exist for **1** and **3**. With use of molecular graphics simulation,[25] a hypothetical isomer II of com-

(23) ^{1}H NMR shifts for Fe–H–B protons are generally relatively insensitive to temperature; hence we would not attribute the observed change in chemical shift to a temperature effect.

(24) The presence of two isomers, which interconvert in solution at room temperature, has been reported for other heteronuclear, gold atom containing clusters, for example, [Ru$_6$(CO)$_{16}$C(AuPEt$_3$)$_2$]: Bunkhall, S. R.; Holden, H. D.; Johnson, B. F. G.; Lewis, J.; Pain, G. N.; Raithby, P. R.; Taylor, M. J. *J. Chem. Soc., Chem. Commun.* **1984**, 25.

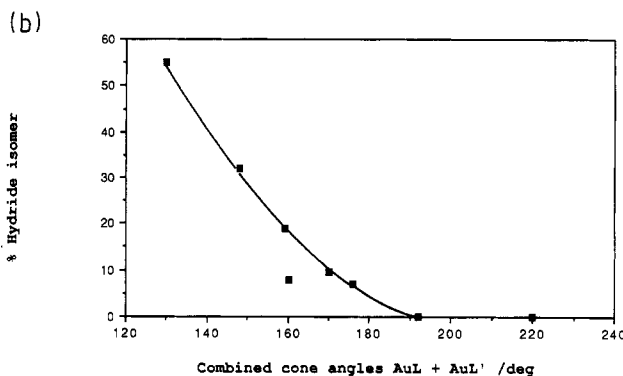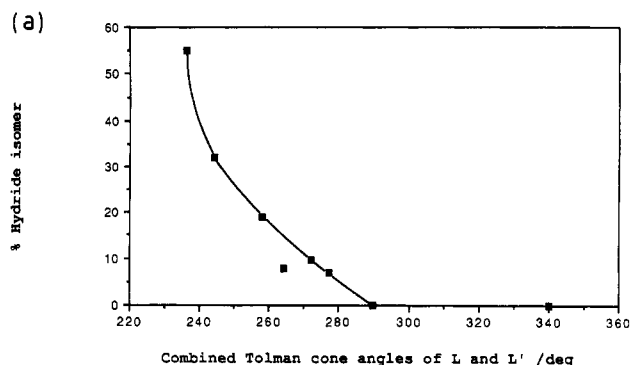(25) *Molecular Editor* distributed by Kinko Academic Courseware Exchange, Santa Barbara, CA 93110.

Figure 6. Space-filling diagram of (a) the hypothetical isomer II and (b) the experimentally observed isomer I of Fe$_4$(CO)$_{12}$Au$_2$[PPh$_3$]$_2$BH. The three operations required to convert II to I are indicated by the arrows.

pound **3** was constructed. The HFe$_4$(CO)$_{12}$Au$_2$P$_2$ framework of **2** was retained, and the ethyl groups of **2** were replaced by phenyl substituents. The geometry of a given PPh$_3$ ligand reflected that found in **3**.[26] The two PPh$_3$ groups were then rotated, each about its respective Au–P bond, such that the model molecule retained C_{2v} symmetry. No positions could be found in which the PPh$_3$ groups simultaneously avoided one another *and* the carbonyl ligands. The best geometry available is shown in Figure 6a. While providing satisfactory minimum phenyl to carbonyl separations of H···OC$_{wing}$ = 2.68 and H···OC$_{hinge}$ = 2.86 Å, respectively,[27] this geometry gives unreasonable interphosphine H···H distances, the shortest of which is 2.29 Å. There is little scope for relieving this strain by moving the PPh$_3$ groups apart. Close approach of the phenyl hydrogen and carbonyl oxygen atoms soon becomes a problem. However, if the movement apart of the PPh$_3$ groups is coupled with a rotation of one hinge Fe(CO)$_3$ unit (Figure 6a), both phosphine···phosphine and phosphine···carbonyl requirements are satisfied. A corollary of the $\approx$60° rotation of the Fe(CO)$_3$ moiety is the creation of a semibridging CO across the Fe$_{hinge}$–Fe$_{hinge}$ bond. This necessitates the migration of the hydride that originally occupied this site (Figure 6a). Once the two AuPPh$_3$ groups have relaxed apart, a site suitable for proton addition opens up along an Fe$_{wing}$–B edge (Figure 6b). While not mechanistically proven, the process described above and shown schematically in Figure 6 does provide one reasonable way in which isomers I and II of compound **2** might interconvert.[28] Clearly, for compounds **1** and **3**, structure I is favored on steric grounds.

Solution Studies of [Fe$_4$(CO)$_{12}$Au$_2$LL'BH] (L = L' = P(c-C$_6$H$_{11}$)$_3$, P(p-C$_6$H$_4$)$_3$, PPh$_3$, PEt$_3$, PMePh$_2$, PMe$_2$Ph, PMe$_3$; L = PPh$_3$, L' = PEt$_3$; L = PMePh$_2$, L' = PMe$_2$Ph). We have presented above the idea that a sterically controlled equilibrium exists between isomers I and II of **2** and that for **1** and **3** only one structure, I, may be tolerated. In order to provide more conclusive evidence for this postulate, we have prepared further members of the series [Fe$_4$(CO)$_{12}$Au$_2$L$_2$BH] (L = P(c-C$_6$H$_{11}$)$_3$, PMePh$_2$, PMe$_2$Ph, PMe$_3$). In addition, the mixed gold(I) phosphine derivative [Fe$_4$(CO)$_{12}$Au$_2$[PMePh$_2$][PMe$_2$Ph]BH] has been prepared and will be considered below along with the previously reported compound [Fe$_4$(CO)$_{12}$Au$_2$[PPh$_3$][PEt$_3$]BH].[18]

Let us consider first the homophosphine complexes. As the cone angle[5,19] of the phosphine substituent decreases,

(26) The "propeller-like" distribution of the phenyl rings in the PPh$_3$ group is a recurrent feature in triphenylphosphine complexes.

(27) Distances are judged to be satisfactory if they are no shorter than the corresponding separations observed in the crystallographically determined structures of **1**, **3**,[1] and Fe$_4$(CO)$_{12}$Au$_3$[PPh$_3$]$_3$B.[4]

(28) Endo-hydrogen migration between Fe$_{wing}$–H–B and Fe$_{hinge}$–H–Fe$_{hinge}$ sites is a known phenomenon.[17]

Table VII. ¹H and ¹¹B NMR Spectroscopic Data and Isomer I and II Distribution for [Fe₄(CO)₁₂Au₂LL'BH]

L	L'	$\delta(^1H)$ (298 K, CD_2Cl_2)	$\delta(^{11}B)$ (298 K, CD_2Cl_2)	% isomer II[a]	II[b]	ref
PPh₃	PPh₃	-9.1	+137.7	0	0	1, 18
P(p-MeC₆H₄)₃	P(p-MeC₆H₄)₃	-9.1	+138.0	0	0	c
P(c-C₆H₁₁)₃	P(c-C₆H₁₁)₃	-9.1	+138.0	0	0	c
PPh₃	PEt₃	-10.2	+140.7	7	6.5	18
PEt₃	PEt₃	-10.4	+142.4	8	11	18
PMePh₂	PMePh₂	-10.6	+141.8	9.5	9	c
PMePh₂	PMe₂Ph	-12.1	+145.5	19	18	c
PMe₂Ph	PMe₂Ph	-14.2	+151.0	32	32	c
PMe₃	PMe₃	-17.8	+163.8	55	63	c

[a] Calculated from ¹H NMR chemical shift data based upon Fe–H–B for structure I at δ -9.1, Fe–H–Fe at δ -24.9. [b] Calculated from ¹¹B NMR chemical shift data based upon $\delta(^{11}B)$ for structure I at +138 and for structure II at +179. [c] This work
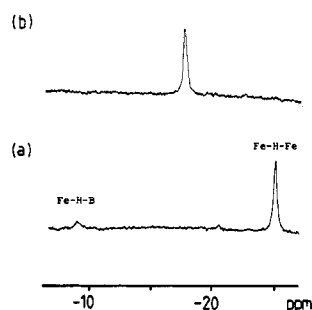
Figure 7. 250-MHz ¹H NMR spectra for [Fe₄(CO)₁₂Au₂-{PMe₃}₂BH], plotted in the region of Fe–H–B and Fe–H–Fe resonances, at (a) 200 K and (b) 298 K.

the ¹H NMR chemical shift for the cluster-bound hydrogen atom moves progressively to higher field as shown in Table VII. The cluster [Fe₄(CO)₁₂Au₂{P(c-C₆H₁₁)₃}₂BH], like 1 and 3, shows a temperature-invariant ¹H NMR signal at δ -9.1. For each of the remaining clusters, cooling to ≈200 K produces two signals, one at δ -9.1 ± 0.1 corresponding to isomer I and the other at δ -24.9 ± 0.1 corresponding to isomer II. The case for L = PMe₃ is illustrated in Figure 7; the fact that the signals at 200 K are still somewhat broad implies that interconversion of the two isomers is not entirely frozen out. The percentage of each isomer present in a CD₂Cl₂ solution at room temperature has been calculated on the basis of the ¹H NMR chemical shifts (Table VII, column 5). The shift in the isomer equilibrium toward structure II reflects the cone angle of the phosphine substituent, as shown graphically in Figure 8a. The cone angle given is the sum of the Tolman cone angles (Table VIII) either for 2L in [Fe₄(CO)₁₂Au₂L₂BH] or for (L + L') in the heterophosphine derivatives [Fe₄(CO)₁₂Au₂LL'BH]. However, the structural change observed in going from isomer I to II obviously depends upon the gold(I) phosphine unit as a whole. Thus, by using a method similar to that of Mingos,[29] we have determined cone angles for each gold(I) phosphine fragment.[30] These values are listed in Table VIII. Figure 8b illustrates the dependence of the

(29) Mingos, D. M. P. *Inorg. Chem.* **1982**, *21*, 464.

(30) Use was made of a molecular graphics package (ref 25) to calculate cone angles for AuL fragments. The validity of this method was first checked by reproducing Tolman cone angles for the phosphine ligands, L. The only phosphines exhibiting conformational flexibility are PEt₃ and P(c-C₆H₁₁)₃. Conformations were chosen so as to reproduce the Tolman cone angle and were then used in the determination of the AuL cone angles. The Au–P distance is 2.28 Å in each AuL fragment. In the auraferraboranes that we have structurally characterized, a typical distance from the Au atom to the center of the Fe–B bond, which it bridges, is 2.3 Å. Thus, for the cone angle of a AuL fragment, we have taken for the apex of the cone, a point that is 2.3 Å away from the Au atom. See ref 19 and 29.

Figure 8. Plot of the percentage of isomer II of [Fe₄-(CO)₁₂Au₂LL'BH] present in solution at room temperature, against (a) the combined Tolman cone angles of the phosphine substituents, L and L', and (b) the combined cone angles for the gold(I) phosphines, AuL and AuL'.[30]

Table VIII. Cone Angles for Phosphines and for Gold(I) Phosphine Fragments

phosphine, L	cone angle, deg L[5,19]	AuL fragment
P(c-C₆H₁₁)₃	170	110
PPh₃	145	96
P(p-MeC₆H₄)₃	145	96
PMePh₂	136	85
PEt₃	132	80
PMe₂Ph	122	74
PMe₃	118	65

isomer equilibrium upon the steric requirements of the gold(I) phosphine groups.

The room-temperature ¹¹B NMR resonances for the compounds [Fe₄(CO)₁₂Au₂LL'BH] are listed in Table VII and range from δ 137.7 for L = L' = P(c-C₆H₁₁)₃ (cone angle = 170°)[5] to δ 163.8 for L = L' = PMe₃ (cone angle = 118°).[5] Since ¹¹B NMR resonances are broad and still broader at low temperatures, it has not been possible to resolve signals for the separate isomers of the compounds [Fe₄-(CO)₁₂Au₂LL'BH] except in the case of the trimethyl- and dimethylphenylphosphine derivatives where both isomers are present in significant amounts. The low-temperature ¹¹B NMR spectra of the latter show two signals. The lower field resonance at δ 179 is assigned to isomer II, and the resonance at δ 138 is assigned to isomer I. The shift difference is consistent with a greater degree of direct metal–boron bonding in isomer II. By using the room-temperature ¹¹B NMR data, we have again estimated the preference for isomer II over isomer I. The results are listed in column 6 of Table VII and compare favorably with those obtained from the ¹H NMR data.

In both the graphs in Figure 8, data for [HFe₄-(CO)₁₂Au₂(PEt₃)₂B] appear to be anomalous. The ob-

served percentage of isomer II present suggests that the AuPEt$_3$ ligand behaves as though it exerts a larger steric effect than would be predicted either by the average Tolman phosphine cone angle or by our calculated gold(I) phosphine cone angle. In solution, this is not surprising, since the alkyl groups of the PEt$_3$ ligand will be flexible, and the cone angle of both PEt$_3$ and AuPEt$_3$ will be subject to error.[15] The Au$_2$(PPh$_3$)(PEt$_3$) moiety will clearly be less flexible than the Au$_2$(PEt$_3$)$_2$ fragment. Thus, data corresponding to [Fe$_4$(CO)$_{12}$Au$_2$(PPh$_3$)(PEt$_3$)BH] are not expected to show significant deviation from the curves shown in Figure 8. The only other phosphine exhibiting conformational variation is P(c-C$_6$H$_{11}$)$_3$. However, the data presented in Figure 8 suggest that the cone angle for P-(c-C$_6$H$_{11}$)$_3$ is past the steric threshold at which the formation of isomer II is allowed. Thus, any variation in the cone angle of P(c-C$_6$H$_{11}$)$_3$ is inconsequential.

Finally, a comment should be made concerning the ^{31}P NMR spectra of the clusters. In the absence of any exchange processes, isomer I should exhibit two phosphorus environments, and for **3**, we have already reported that this is indeed the case. Each of the compounds [Fe$_4$-(CO)$_{12}$Au$_2$LL'BH] (L = L' = P(c-C$_6$H$_{11}$)$_3$, P(p-MeC$_6$H$_4$)$_3$, PPh$_3$, PEt$_3$, PMePh$_2$, PMe$_2$Ph, PMe$_3$; L = PMePh$_2$, L' = PMe$_2$Ph) shows only one ^{31}P NMR resonance at room temperature. This in itself comes as no surprise, since the ability of a heteronuclear cluster involving gold(I) phosphine units to undergo transition-metal–gold bond cleavage leading to rearrangement of the cluster core has previously been observed.[31] However, we expected that, upon cooling, if a fluxional process were frozen out, we should observe the presence of both isomers I and II of [Fe$_4$-(CO)$_{12}$Au$_2$LL'BH]. In each case, however, only *two* ^{31}P NMR resonances were observed at ≈200 K. As reported for **3**,[18] the integrals of the low-temperature ^{31}P NMR signals for **1** and [Fe$_4$(CO)$_{12}$Au$_2$[P(c-C$_6$H$_{11}$)$_3$]$_2$BH] were in the ratio 1:1, thereby consistent with the presence of one isomer, viz. isomer I. For the remaining compounds, with the exception of [Fe$_4$(CO)$_{12}$Au$_2$[PEt$_3$]$_2$BH][18] and [Fe$_4$-(CO)$_{12}$Au$_2$[PEt$_3$][PPh$_3$]BH],[18] the ratio of the intensities of the two low-temperature signals varied, with the higher field resonance being of a greater intensity than the lower field one. These data may be rationalized if one assumes that, for isomer II, the environment of the phosphorus atom very closely matches that of one of the phosphorus atoms in isomer I. This is reasonable, since, in isomer II, both gold(I) phosphine units bridge Fe$_{wing}$–B edges and, in isomer I, *one* gold(I) phosphine fragment mimics this bonding mode. We suggest, therefore, that the ^{31}P NMR resonance of isomer II coincides with one of the signals for isomer I but that for [Fe$_4$(CO)$_{12}$Au$_2$[PEt$_3$][PPh$_3$]BH] in particular, the contribution made by isomer II is too small to allow detection of both isomers in the ^{31}P NMR spectra.

Conclusion. The cluster [Fe$_4$(CO)$_{12}$Au$_2$LL'BH] may exist in one of two isomeric forms depending upon the steric requirements of the gold(I) phosphine fragments. In structure I, the boron atom retains a boron–hydrogen interaction, and the cluster exhibits an asymmetrical array of metal atoms. In structure II, the boron atom is naked and resides within a more symmetrical (though nonoctahedral), six metal atom cage. For phosphines with a Tolman cone angle ≥145°, only structure I is sterically allowed. For smaller phosphines, a solution eqilibrium exists between the two isomers, and the equilibrium constant shows a clear dependence upon the steric requirements of the gold(I) phosphine fragments. In both isomers I and II, the AuL groups aggregate about the boron atom, and there is no evidence for further isomers in which a gold(I) phosphine group bridges the Fe$_{hinge}$–Fe$_{hinge}$ bond of the tetrairon atom butterfly framework. This cannot be explained in steric terms, since such a bonding mode has previously been exemplified in the [Fe$_4$(CO)$_{13}$(Au-PEt$_3$)]$^-$ anion.[32] Thus, we suggest that the heavy metal phosphine moieties are driven toward the boron atom by electronic factors. We have previously illustrated that interaction with an Fe–B rather than an Fe–Fe bond allows the gold atom to attain a more favorable charge distribution.[1]

Finally, there is an upper limit for the size of the phosphine ligand in the cluster [Fe$_4$(CO)$_{12}$Au$_2$LL'BH]. Attempts to prepare [Fe$_4$(CO)$_{12}$Au$_2$[P(o-MeC$_6$H$_4$)$_3$]$_2$BH] have so far failed, and the reaction of [HFe$_4$(CO)$_{12}$BH]$^-$ with excess P(o-MeC$_6$H$_4$)$_3$ leads only to a monogold derivative.[33] The cone angle, θ, for P(o-MeC$_6$H$_4$)$_3$ is 194°,[5] and thus we may state that for the direct synthesis of the auraferraborane cluster [Fe$_4$(CO)$_{12}$Au$_2$L$_2$BH], the steric constraint upon L is such that $170 \leq \theta_{max} \leq 194°$.

(31) See for example: Freeman, M. J.; Orpen, A. G.; Salter, I. D. *J. Chem. Soc., Dalton Trans.* **1987**, 379. Farrugia, L. J.; Freeman, M. J.; Green, M.; Orpen, A. G.; Stone, F. G. A.; Salter, I. D. *J. Organomet. Chem.* **1983**, *249*, 273. Bateman, L. W.; Green, M.; Mead, K. A.; Mills, R. M.; Salter, I. D.; Stone, F. G. A.; Woodward, P. *J. Chem. Soc., Dalton Trans.* **1983**, 2599. Howard, J. A. K.; Salter, I. D.; Stone, F. G. A. *Polyhedron* **1984**, *3*, 567. Bateman, L. W.; Green, M.; Howard, J. A. K.; Mead, K. A.; Mills, R. M.; Salter, I. D.; Stone, F. G. A.; Woodward, P. *J. Chem. Soc., Chem. Commun.* **1982**, 773.

(32) Horowitz, C. P.; Holt, E. M.; Brock, C. P.; Shriver, D. F. *J. Am. Chem. Soc.* **1985**, *107*, 8136.

(33) Housecroft, C. E.; Shongwe, M. S.; Rheingold, A. L., manuscript in preparation.